RAA 2018 Vol. **18** No. **11**, 139(8pp) doi: 10.1088/1674–4527/18/11/139

http://www.raa-journal.org *http://iopscience.iop.org/raa*

Research in Astronomy and Astrophysics

The first CCD photometric study of the open cluster NGC 744

Kun Wang[1], Li-Cai Deng[1,2], Zhi-Quan Luo[1], Zheng-Zhou Yan[1], Qi-Li Liu[3], Jin-Jiang Sun[3] and Qiang Zhou[3]

[1] Department of Astronomy, China West Normal University, Nanchong 637009, China; *kwang@cwnu.edu.cn*
[2] Key Laboratory of Optical Astronomy, National Astronomical Observatories, Chinese Academy of Sciences, Beijing 100101, China
[3] Purple Mountain Observatory, Chinese Academy of Sciences, Nanjing 210008, China

Received 2018 April 18; accepted 2018 May 30

Abstract We present the first CCD photometric observations of open cluster NGC 744, as part of the 50BiN Open Cluster Survey. The color-magnitude diagrams of this cluster were derived from absolute $BVRI$ photometry on a good photometric night. A brief isochrone fitting gives a distance modulus of $(m-M)_V = 11.58 \pm 0.2$ and a reddening of $E(B-V) = 0.35 \pm 0.05$ with an age of $\log t = 8.30 \pm 0.05$. By carefully examining the BV time-series data, we discovered four new variable stars in a $20' \times 20'$ field around the cluster. We classified them as three eclipsing binary stars and one δ Scuti pulsating star, mainly based on the light-curve shape, the detected periods and the positions on the color-magnitude diagrams.

Key words: open clusters and associations: individual (NGC 744) — stars: variables: general

1 INTRODUCTION

Open clusters are gravitationally bound stellar systems containing from several hundred to tens of thousands of coeval stars with nearly the same distance and chemical composition (Kalirai & Richer 2010; de Grijs 2010; Friel 2013). They have served as ideal laboratories for the study of a vast array of astrophysical phenomena on many scales. Since open clusters provide valuable information about fundamental physical parameters (age, reddening, metallicity and distance) of stars in the cluster, they are excellent targets to understand stellar interiors and evolution. Besides, open clusters are found at almost all locations in the Galactic disk, making them superb tracers of Galactic structure and evolution. Most kinds of variable stars are discovered in open clusters, and such variable stars provide an ideal opportunity to test the stellar theoretical models and explore some important physical processes such as mass transfer and common-envelope evolution (Jiang et al. 2009; Ivanova et al. 2013).

Although there are about 2000 open clusters in the catalog of Dias et al. (2002), only ≈400 clusters have been studied by modern high quality CCD observations (Netopil et al. 2012). We have started the 50 cm Binocular Network (50BiN) Open Cluster Survey (Deng et al. 2013; Wang et al. 2015; Tian et al. 2016), a project dedicated to providing homogeneous photometry of a sample of Galactic open clusters using the 50BiN. The primary science goals are to determine fundamental physical parameters of a large number of open clusters and perform studies of stellar variability in selected open clusters. In this paper we report the results of the open cluster NGC 744, with coordinates $\alpha_{\rm J2000} = 01^{\rm h}58^{\rm m}36.0^{\rm s}$, $\delta_{\rm J2000} = +55^\circ28'00''$ (Kharchenko et al. 2005).

NGC 744 is a poorly studied open cluster and has no CCD photometry so far. The Catalogue of Open Cluster Data lists the basic parameters of this cluster as: $E(B-V) = 0.381$, $\log(t) = 8.375$ and $(m_{Ks} - M_{Ks})$ = 10.825 (Kharchenko et al. 2013). This paper is organized as follows. In Section 2, we present the observations and data reductions. The photometric calibration and cluster parameters are investigated in Section 3. The variable selection procedures and their physical properties are discussed in Section 4 and a brief summary is given in Section 5.

2 OBSERVATIONS AND DATA REDUCTION

All images analyzed in this paper were collected with the 50 centimeter binocular telescope (50BiN prototype telescope) at Qinghai Station of Purple Mountain Observatory, Chinese Academy of Sciences. This telescope employs a binocular equatorial mount system and has two parallel camera systems. Each of them is equipped with an Andor 2048×2048 pixel CCD, resulting in an image scale of about $0.59''$ pixel^{-1} and a $20' \times 20'$ field of view. Details of this telescope can be found at the website (*http://song.bao.ac.cn*).

Time-series observations were performed on 13 nights from 2015 October 15 to November 3. Two standard Johnson BV filters, incorporated in the two camera systems respectively, were used for simultaneous two-color photometry. The time-series observing log is presented in Table 1. Image reduction was done with an automated reduction pipeline (Wang et al. 2015), which is mainly based on DAOPHOT II (Stetson 1992). The main steps include bias subtraction, flat-fielding, astrometry and photometry extraction.

We took calibration images on the night of 2016 February 1 under photometric conditions. Two sets of standard Johnson-Cousins-Bessell $BVRI$ filters, installed on the two parallel camera systems respectively, were used for photometry. A total of ten standard stars in two Landolt standard fields SA20 SF4 and SA23 SF1 (Landolt 2013) were observed to derive the transformation equations between the instrumental and standard systems. These stars have a color range of 0.09 $\leq (B-V) \leq$ 1.88. The details of $BVRI$ observations are provided in Table 2. Aperture photometry was done on the standard star frames by using the associated IRAF tasks and packages[1]. Point-spread function (PSF) photometry of the target images was carried out with an automated reduction pipeline, just like the previous time-series data processing. Frame-by-frame aperture corrections were determined by computing the differential magnitude between the PSF and aperture photometry of 55 relatively bright, isolated stars in the cluster frame. These corrections were then applied to the original PSF photometry.

[1] Image Reduction and Analysis Facility (IRAF) is distributed by the National Optical Astronomy Observatories.

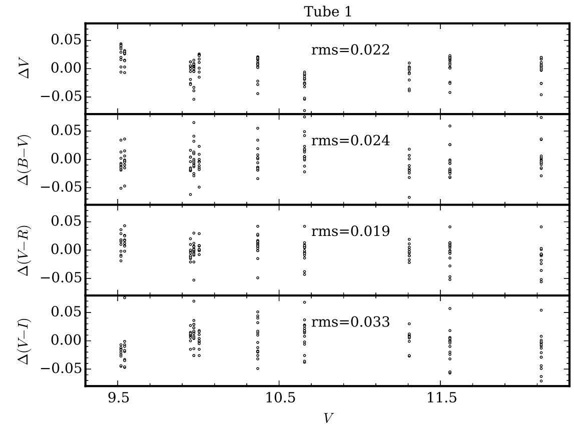

Fig. 1 Star-by-star comparison of our observed photometry from Tube 1 with Landolt (2013) catalog values.

3 PHOTOMETRIC STUDY OF THE OPEN CLUSTER NGC 744

3.1 Photometric Calibration

The PHOTCAL package within IRAF was applied to construct the following transformation equations:

$$b = B + c_1 + k_b X + m_1(B - V)\,, \tag{1}$$

$$v = V + c_2 + k_v X + m_2(B - V)\,, \tag{2}$$

$$r = R + c_3 + k_r X + m_3(V - R)\,, \tag{3}$$

$$i = I + c_4 + k_i X + m_4(V - I)\,, \tag{4}$$

where B, V, R and I represent the standard magnitudes, b, v, r and i are the instrumental magnitudes, and X is the airmass. The coefficient values, including zero points, extinction and color terms, are reported in Table 3.

Figures 1 and 2 display the differences between transformed magnitudes and colors of standard stars and the Landolt (2013) catalog values. Tube 1 has a photometric solution with root mean square (rms) of $\approx$ 0.02 mag in BVR and ≈ 0.03 in I while Tube 2 shows a better photometric solution with rms less than 0.015 mag per filter. In addition, a comparison between the two tubes is displayed in Figure 3.

3.2 Comparison with Previous Photometry

Instrumental magnitudes of NGC 744 in $BVRI$ bands were transformed into the standard system by using the transformation Equations (1)–(4) above. Stars that were

Table 1 Log of Time-series Observations for NGC 744

Date	Start (HJD 2457300+)	Length (h)	Exp. (in seconds) (B, V)	Frames (B, V)
2015 Oct 15	11.056	8.2	70, 30	374, 840
2015 Oct 18	14.201	4.8	70, 30	218, 502
2015 Oct 21	17.105	7.0	100, 50	230, 405
2015 Oct 22	18.001	9.3	100, 50	288, 582
2015 Oct 23	19.100	6.7	100, 50	203, 439
2015 Oct 24	20.107	6.6	100, 50	201, 531
2015 Oct 26	22.003	9.0	100, 50	284, 542
2015 Oct 28	23.987	9.2	100, 50	289, 527
2015 Oct 29	25.012	1.7	100, 50	39, 83
2015 Oct 30	26.010	8.5	100, 50	210, 409
2015 Nov 01	28.062	7.0	100, 50	235, 445
2015 Nov 02	29.053	8.1	100, 50	274, 525
2015 Nov 03	30.008	5.8	100, 50	177, 367

Table 2 Log of $BVRI$ Observations

Tube	Object	B ($n\times$ Exp.)	V ($n\times$ Exp.)	R ($n\times$ Exp.)	I ($n\times$ Exp.)	Airmass
Tube 1	NGC 744	4×200	4×100	4×70	4×70	1.16–1.24
...	...	4×40	4×20	4×10	4×20	1.16–1.25
...	SA20 SF4	12×20	12×10	12×7	12×10	1.24–1.69
...	SA23 SF1	16×30	16×15	16×8	16×10	1.00–1.07
Tube 2	NGC 744	4×200	4×100	4×70	4×70	1.16–1.24
...	...	4×40	4×20	4×10	4×20	1.16–1.25
...	SA20 SF4	12×20	12×10	12×7	12×10	1.24–1.69
...	SA23 SF1	16×30	16×15	16×8	16×10	1.00–1.07

Table 3 Coefficients of the Calibration Equations

Tube	Zero point	Extinction	Color Term	rms
Tube 1	$c_1 = 3.741 \pm 0.007$	$k_b = 0.286 \pm 0.005$	$m_1 = -0.034 \pm 0.002$	0.015
...	$c_2 = 3.386 \pm 0.009$	$k_v = 0.196 \pm 0.007$	$m_2 = 0.021 \pm 0.003$	0.021
...	$c_3 = 3.363 \pm 0.007$	$k_r = 0.138 \pm 0.005$	$m_3 = 0.114 \pm 0.004$	0.016
...	$c_4 = 4.793 \pm 0.017$	$k_i = 0.131 \pm 0.012$	$m_4 = 0.070 \pm 0.004$	0.034
Tube 2	$c_1 = 3.774 \pm 0.007$	$k_b = 0.298 \pm 0.005$	$m_1 = -0.047 \pm 0.002$	0.015
...	$c_2 = 3.468 \pm 0.006$	$k_v = 0.214 \pm 0.004$	$m_2 = -0.003 \pm 0.002$	0.014
...	$c_3 = 3.388 \pm 0.007$	$k_r = 0.166 \pm 0.005$	$m_3 = 0.067 \pm 0.004$	0.015
...	$c_4 = 4.687 \pm 0.011$	$k_i = 0.141 \pm 0.008$	$m_4 = 0.031 \pm 0.003$	0.023

detected in at least two images were averaged. Since this cluster has not been intensively observed in the past, we just compared our results with the UCAC4[2] catalog (Zacharias et al. 2013) and APASS[3] catalog (Henden et al. 2016). Due to a higher photometric accuracy, the photometric data derived from Tube 2 were used to conduct the comparison. Such a comparison is shown in Figure 4 where we plot the differences ΔV and $\Delta(B-V)$ as a function of V magnitude from the present study.

[2] UCAC4 represents the fourth United States Naval Observatory (USNO) CCD Astrograph Catalog.

[3] APASS stands for the AAVSO Photometric All Sky Survey.

The comparison indicates that the $(B-V)$ colors and V magnitudes obtained in the present work are in general in agreement with those provided by APASS and UCAC4. The mean differences with those stars brighter than $V \leq 14$ mag were calculated as follows:

$$\Delta V_{\rm APASS} = 0.03 \pm 0.04,$$

$$\Delta(B-V)_{\rm APASS} = -0.02 \pm 0.03,$$

$$\Delta V_{\rm UCAC4} = 0.03 \pm 0.07,$$

and

$$\Delta(B-V)_{\rm UCAC4} = -0.05 \pm 0.10.$$

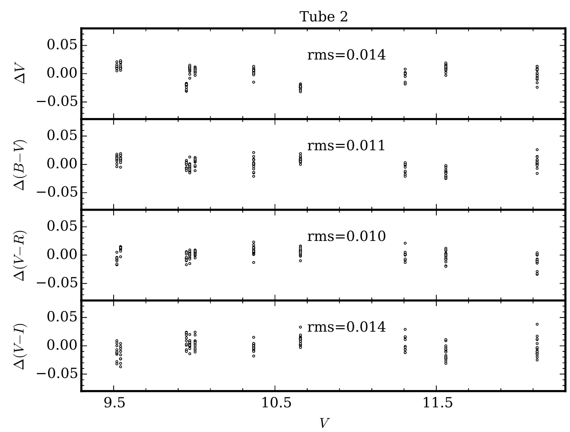

Fig. 2 Star-by-star comparison of our observed photometry from Tube 2 with Landolt (2013) catalog values.

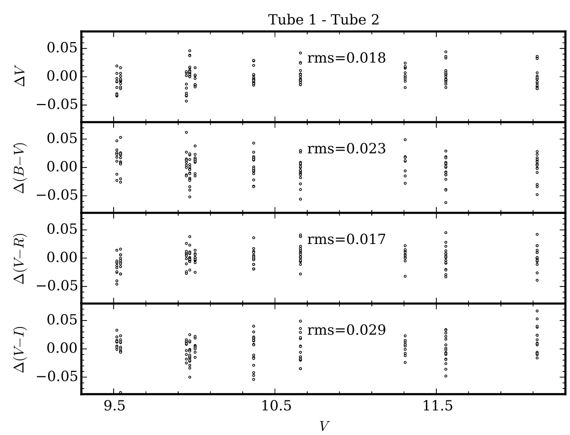

Fig. 3 Star-by-star photometry comparison between Tube 1 and Tube 2.

3.3 Color-Magnitude Diagrams

The standard magnitudes given by Tube 2 were used to construct the color-magnitude diagrams (CMDs). The three panels of Figure 5 display the CMDs of NGC 744 in the $B-V$, $V-R$ and $V-I$ passbands. The physical parameters of the cluster were estimated by fitting isochrones to the CMDs (Bressan et al. 2012), assuming a solar metallicity abundance ($Z = 0.019$). The fitting has been done with the traditional visual screening approach. By using the Padova evolutionary code (Bressan et al. 2012), we made a sequence of isochrones with constant metallicity, $Z = 0.019$, from $\log(t/\mathrm{yr}) = 7.5$ to 9 in steps of 0.05. The reddening value $E(B-V)$ was set to be within 0.25–0.45 with step size 0.05. The distance modulus $(m-M)_o$ varied in the range from 9.5 to 11.5 with step size 0.2. The fitting is verified by a visual comparison between the theoretical isochrone and the CMDs. The main sequence and one evolved star, TYC 3688-1931-1, were treated as criteria in the fitting procedures. The membership probabilities from proper motion, photometry and spatial position all suggest that TYC 3688-1931-1 could be a member of NGC 744 (Kharchenko et al. 2004). Based on many trials, we obtained a reasonable fitting. The best-fitting theoretical results of the cluster are: age $\log t = 8.30 \pm 0.05$, reddening value $E(B-V) = 0.35 \pm 0.05$ mag and distance modulus $(m-M)_V$ = 11.58±0.2. All errors were taken from the step size. These results are in modest agreement with Kharchenko et al. (2013).

4 VARIABLE STARS IN THE OPEN CLUSTER NGC 744

4.1 Identification of Variable Stars

An ensemble normalization technique (Gilliland & Brown 1988) was applied to calibrate instrumental magnitudes of the time-series BV frames. About 40 isolated bright stars that showed long-term stability during the observations were selected to determine the following transformation equation

$$V = v + a_1 + a_2(B-V) + a_3X + a_4Y \ , \qquad (5)$$

where X and Y are the star positions in a CCD frame. The coefficients a_1, a_2, a_3 and a_4 whose values are different for each frame were determined by using the 40 selected stars. An identical equation was applied to the B time-series images. For each frame, the instrumental magnitudes v were then calibrated to the standard magnitudes V using the above equation and the mid-exposure time was converted to Heliocentric Julian Date (HJD). The time-series light curve of an individual star was extracted in this way.

Following the same procedure used by Wang et al. (2015), the light variabilities of all detected stars were examined. Firstly, the Stetson variability index J (Stetson 1996) for each star was calculated with simultaneous B- and V-band light curves. Stars with variability indices J less than 0.4 (Zhang et al. 2003) were rejected. We then carefully examined the light variations of each variable candidate by visual inspection and identified four clearly variable stars, all of which are new discoveries. They are labeled as $V1$, $V2$, $V3$ and $V4$, ordered by V magnitude.

Figure 6 shows the observed CCD field of the open cluster with the detected variables marked. The main parameters of these variables are given in Table 4. The

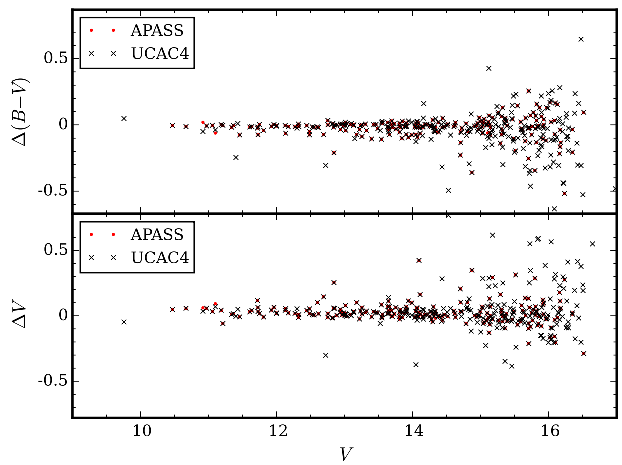

Fig. 4 Comparison of the present photometry with data in the UCAC4 catalog and APASS catalog.

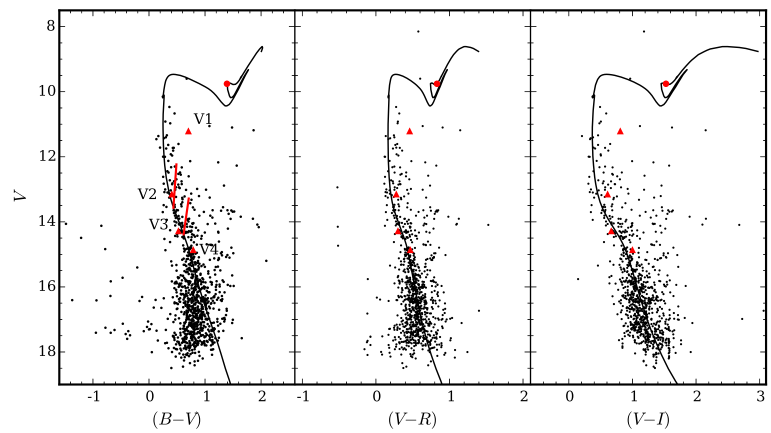

Fig. 5 The CMDs $B-V$, $V-R$ and $V-I$ as a function of V for stars in the field of NGC 744. The dark solid lines represent the Padova theoretical isochrone (Bressan et al. 2012) with cluster parameters ($\log t = 8.30$, $Z = 0.019$, $E(B-V) = 0.35$ and $(m-M)_V$ = 11.58). The *red triangular symbols* and the *big red dot* denote variable stars and evolved star TYC 3688-1931-1, respectively. The *red solid lines* are the borders of the instability strip for δ Scuti (Breger 1979).

coordinates, V magnitude and colors for the stars were computed from the current photometry. The periods of variable stars were estimated by using a package of computer programs (Period04, Lenz & Breger (2005)) and the phase dispersion minimization (PDM) method (Stellingwerf 1978). Their classifications are given in the last column and will be discussed in detail in the following section.

4.2 Classification and Discussion

The variable stars were classified based on the behaviors of their light curves, detected periods and positions in the CMDs. Details about their classifications are as follows:

V1: This is likely to be an eclipsing binary with an orbital period of 0.3416 days. Its phased light curves are shown in Figure 7. It presents an obvious EB-type light curve in both bands. The light curves display an amplitude of about 0.1 mag, suggesting a low inclination. Ammons et al. (2006) estimated an effective temperature for this star to be about 5693 K. This star lies far away from the isochrone in the CMDs and its proper-motion probability (PMP) was calculated to be zero (Sampedro et al. 2017; Kharchenko et al. 2004). This suggests that V1 could be a non-member of the cluster, although it is located within the central area of the cluster.

V2: An eclipsing binary with an EW-type light curve, as displayed in Figure 7. Its orbital period is about

Table 4 Variable Stars Detected in the NGC 744 Field

Star ID	α_{2000}	δ_{2000}	V (mag)	$B-V$ (mag)	$V-R$ (mag)	$V-I$ (mag)	P (d)	T_0 (d)	Type
V1	01:58:29.10	+55:26:46.30	11.211	0.703	0.459	0.809	0.3416	11.2602	EB
V2	01:58:01.15	+55:28:10.03	13.150	0.408	0.277	0.610	0.6180	29.3265	EW
V3	01:57:34.63	+55:31:46.38	14.281	0.525	0.300	0.667	0.0505		δ Scuti
V4	01:59:30.03	+55:31:55.43	14.861	0.789	0.468	1.000	0.8651	14.2731	EA

Note: T_0 (HJD–2457300) denotes the phase zero epoch.

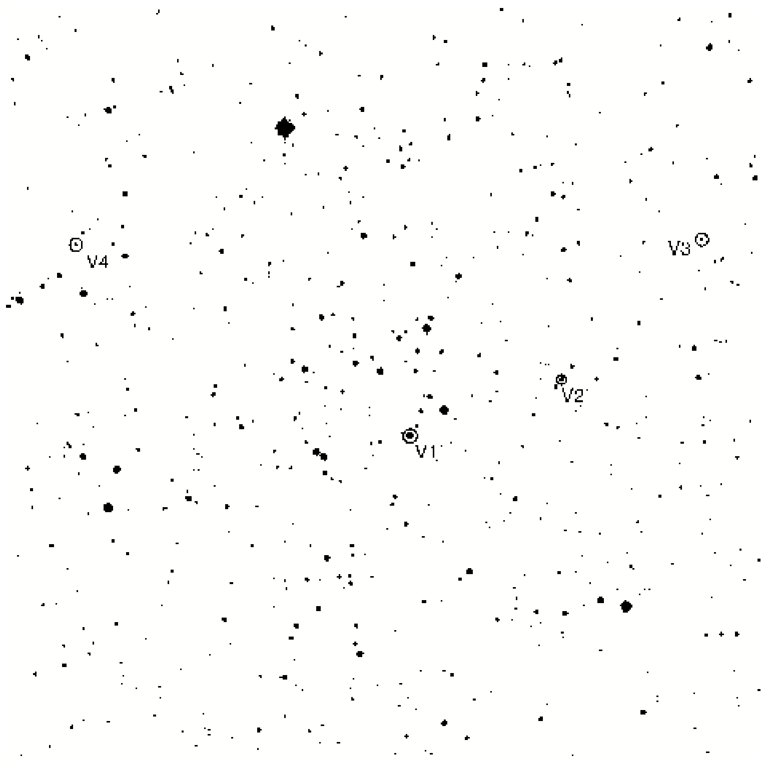

Fig. 6 The field of NGC 744 observed from 50BiN with the four variable stars marked. North is up and east is to the left.

0.6180 days with an amplitude of 0.15 mag. The observed color of the system, $B-V=0.408$, is consistent with the spectral type F0III (Pickles & Depagne 2010). It could be a W UMa star. Although its membership probability from proper motion is calculated to be 0.24, both photometric and spatial cluster membership are higher than 0.98 (Kharchenko et al. 2004). In this case, this star may be a member of the cluster.

V3: A δ Scuti star. The light curves in Figure 8 show rapid light variations with amplitude and cycle length characteristic of δ Scuti-like oscillations. Following Breger et al. (1993) and Wang et al. (2015), a power spectrum analysis was made with the algorithm Period04 consisting of iterative prewhitening steps. The Fourier analysis only detected one dominant frequency of 19.8143 c/d with amplitude signal-to-noise ratio (S/N) higher than 4.0 in both filters, although the star seems to be multiperiodic (see Fig. 8). The amplitude spectra of V3 are depicted in Figure 9. The star is likely to be a cluster member, although there are no PMP data available, since its location in the CMDs is within the δ Scuti instability strip (Breger 1979).

V4: The phased light curves are seen in Figure 7. The shape of the light curves exhibits typical EA-type light variability, with deep primary minima and flat bright parts. The orbital period of this star is estimated as 0.8651 days. There are no proper-motion data available for the star. Its position in the CMDs is very close to the isochrone while located far away from the cluster center. We cannot draw any conclusion about its membership at present.

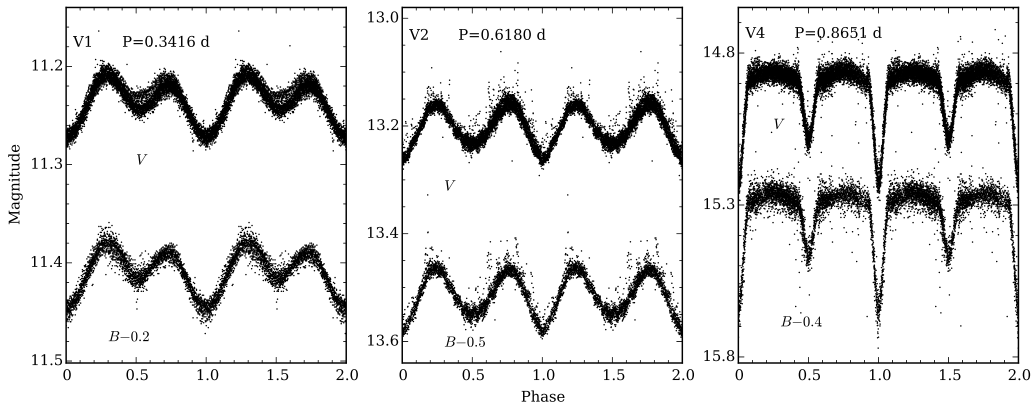

Fig. 7 Phased light curves of the variable stars V1, V2 and V4.

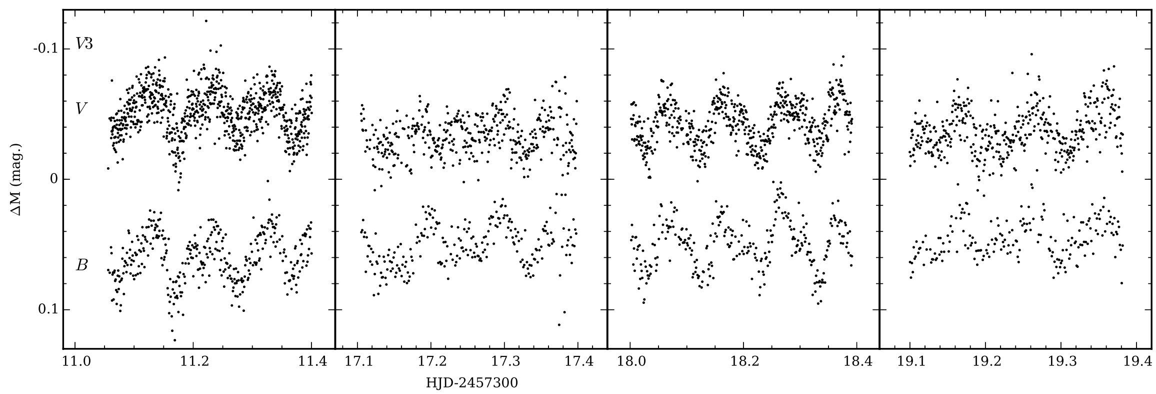

Fig. 8 Sections of the original real-time B- and V-band light curves of the pulsating star V3.

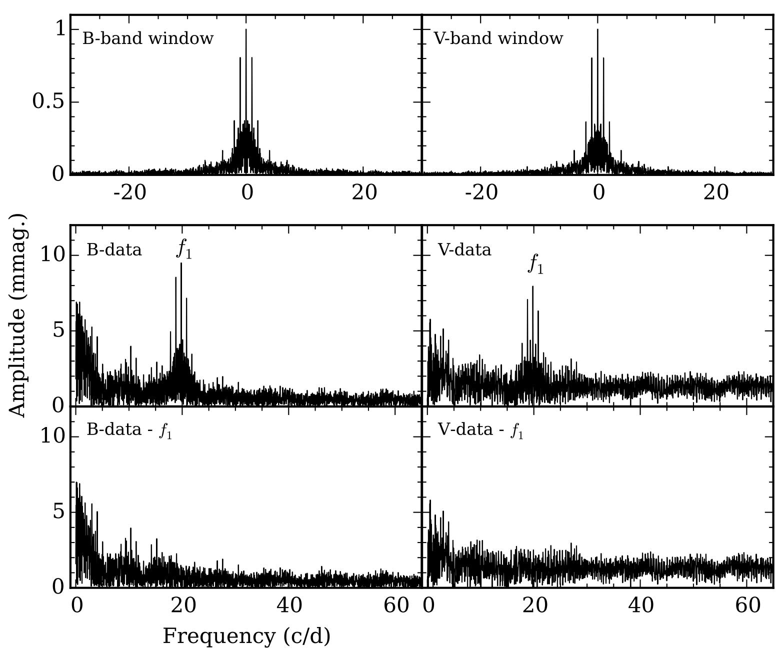

Fig. 9 Spectral windows and amplitude spectra of the pulsating star V3.

5 SUMMARY

In this paper, we reported the first CCD photometric study of the northern open cluster NGC 744. The multicolor $BVRI$ CCD photometry revealed the main characteristics of this cluster and time-series BV observations led to the discovery of four new variable stars. The main results of this research are the following:

(1) By performing standard photometric methods, we have constructed the CMDs of NGC 744 in the $B-V$, $V-R$, and $V-I$ passbands. With a brief isochrone fitting to the CMDs, the physical parameters of the cluster were estimated as follows:

$$(m-M)_V = 11.58 \pm 0.2,$$

$$E(B-V) = 0.35 \pm 0.05,$$

and $\log t = 8.30 \pm 0.05$.

(2) We have discovered four new variable stars in this survey. Three were classified as eclipsing binary systems (V1, V2 and V4) with an EB-type star, an EW-type star and an EA-type star respectively. One δ Scuti pulsating star (V3) was detected.

Acknowledgements This work is supported by the Meritocracy Research Funds of China West Normal University and the Fundamental Research Funds of China West Normal University.

References

Ammons, S. M., Robinson, S. E., Strader, J., et al. 2006, ApJ, 638, 1004
Breger, M. 1979, PASP, 91, 5
Breger, M., Stich, J., Garrido, R., et al. 1993, A&A, 271, 482
Bressan, A., Marigo, P., Girardi, L., et al. 2012, MNRAS, 427, 127
de Grijs, R. 2010, Philosophical Transactions of the Royal Society of London Series A, 368, 693
Deng, L., Xin, Y., Zhang, X., et al. 2013, in IAU Symposium, 288, Astrophysics from Antarctica, eds. M. G. Burton, X. Cui, & N. F. H. Tothill, 318
Dias, W. S., Alessi, B. S., Moitinho, A., & Lépine, J. R. D. 2002, A&A, 389, 871
Friel, E. D. 2013, Planets, Stars and Stellar Systems. Volume 5: Galactic Structure and Stellar Populations, 5, 347
Gilliland, R. L., & Brown, T. M. 1988, PASP, 100, 754
Henden, A. A., Templeton, M., Terrell, D., et al. 2016, VizieR Online Data Catalog, 2336
Ivanova, N., Justham, S., Chen, X., et al. 2013, A&A Rev., 21, 59
Jiang, D., Han, Z., Jiang, T., & Li, L. 2009, MNRAS, 396, 2176
Kalirai, J. S., & Richer, H. B. 2010, Philosophical Transactions of the Royal Society of London Series A, 368, 755
Kharchenko, N. V., Piskunov, A. E., Röser, S., Schilbach, E., & Scholz, R.-D. 2004, Astronomische Nachrichten, 325, 740
Kharchenko, N. V., Piskunov, A. E., Röser, S., Schilbach, E., & Scholz, R.-D. 2005, A&A, 438, 1163
Kharchenko, N. V., Piskunov, A. E., Schilbach, E., Röser, S., & Scholz, R.-D. 2013, A&A, 558, A53
Landolt, A. U. 2013, AJ, 146, 131
Lenz, P., & Breger, M. 2005, Communications in Asteroseismology, 146, 53
Netopil, M., Paunzen, E., & Stütz, C. 2012, Astrophysics and Space Science Proceedings, 29, 53
Pickles, A., & Depagne, É. 2010, PASP, 122, 1437
Sampedro, L., Dias, W. S., Alfaro, E. J., Monteiro, H., & Molino, A. 2017, MNRAS, 470, 3937
Stellingwerf, R. F. 1978, ApJ, 224, 953
Stetson, P. B. 1992, in Astronomical Society of the Pacific Conference Series, 25, Astronomical Data Analysis Software and Systems I, eds. D. M. Worrall, C. Biemesderfer, & J. Barnes, 297
Stetson, P. B. 1996, PASP, 108, 851
Tian, J. F., Deng, L. C., Zhang, X. B., et al. 2016, PASP, 128, 105003
Wang, K., Deng, L., Zhang, X., et al. 2015, AJ, 150, 161
Zacharias, N., Finch, C. T., Girard, T. M., et al. 2013, AJ, 145, 44
Zhang, X.-B., Deng, L.-C., Xin, Y., & Zhou, X. 2003, ChJAA (Chin. J. Astron. Astrophys.), 3, 151